

Scalable Spin Squeezing in Power-Law Interacting XXZ Models with Disorder

Samuel E. Begg,^{1,*} Bishal K. Ghosh,^{1,2} Chong Zu,^{3,4} Chuanwei Zhang,^{3,4} and Michael Kolodrubetz¹

¹*Department of Physics, The University of Texas at Dallas, Richardson, Texas 75080, USA*

²*Institute of Physics, University of Graz, Universitätsplatz 5, 8010 Graz, Austria*

³*Department of Physics, Washington University, St. Louis, Missouri 63130, USA*

⁴*Center for Quantum Leaps, Washington University, St. Louis, Missouri 63130, USA*

(Dated: January 16, 2026)

While spin squeezing has been traditionally considered in all-to-all interacting models, recent works have shown that spin squeezing can occur in systems with power-law interactions, leading to direct testing in Rydberg atoms, trapped ions, ultracold atoms and nitrogen vacancy (NV) centers in diamond. For the latter, Ref. [1] demonstrated that spin squeezing is heavily affected by positional disorder, reducing any capacity for a practical squeezing advantage, which requires scalability with the system size. In this Letter we explore the robustness of spin-squeezing in two-dimensional lattices with a fraction of unoccupied lattice sites. Using semi-classical modeling, we demonstrate the existence of scalable squeezing in power-law interacting XXZ models up to a disorder threshold, above which squeezing is not scalable. We produce a phase diagram for scalable squeezing, and explain its absence in the aforementioned NV experiment. Our work illustrates the maximum disorder allowed for realizing scalable spin squeezing in a host of quantum simulators, highlights a regime with substantial tolerance to disorder, and identifies controlled defect creation as a promising route for scalable squeezing in solid-state systems.

Quantum simulators now provide opportunities for engineering collective quantum phenomena with applications to quantum metrology [2, 3]. A paradigmatic example is spin squeezing [4–6], whereby the quantum projection noise is reduced (squeezed) in a particular direction, which can be exploited to perform precision measurements. While spin squeezing has been traditionally considered in all-to-all interacting models [5, 7], recent works have shown that scalable spin squeezing – where squeezing scales with system size – is possible in systems with power-law interactions [8, 9]. In particular, dynamics thermalizing to the easy-plane ferromagnetic phase display scalable spin squeezing [10], establishing a link between dynamical scaling of quantum information and equilibrium order. Subsequent work has generalized this to the case of quasi-long range ordered phases [11]. The squeezing dynamics can also be partially understood from the perspective of gap-protection of a collective large-spin (Dicke) manifold [9, 12, 13], in which states undergo dynamics qualitatively similar [10] to one-axis-twisting (OAT), the simplest form of spin squeezing. This intuition has motivated generalizations to two-mode squeezing [14–16] and two-axis counter-twisting [17].

The ubiquity of power-law interacting systems in quantum simulators has led to recent demonstrations of spin squeezing in Rydberg atoms [18–20], trapped ions [21], neutral atoms with contact [22] and long-range interactions [23], and nitrogen vacancy (NV) centers in diamond [1]. Hamiltonians capable of spin squeezing have also been realized in polar molecules [24] and cavity-mediated (all-to-all) interactions [25]. For the NV experiment in Ref. [1], squeezing was shown to be significantly affected by positional disorder of the spins, and was not scalable, despite experimental methods for removing strongly interacting spins which reduce collective behavior. Simi-

larly, spin squeezing in three-dimensional optical lattices has been shown to be impacted by a finite hole fraction [22]. A systematic understanding of the robustness of scalable spin squeezing to disorder is currently lacking.

In this Letter we characterize the impact of disorder on spin-squeezing by considering regular two-dimensional (2D) lattices with a fraction p of randomly positioned unoccupied lattice sites (vacancies). Using semi-classical modeling, we demonstrate the existence of scalable squeezing in power-law interacting XXZ models up to a disorder threshold, above which the squeezing is not scalable. The transition is found to align with a change in the presence/absence of order at late times, as anticipated from the U(1) symmetry [10]. Our work illustrates a minimal disorder requirement for realizing scalable spin squeezing in a host of quantum simulators, and explains why Ref. [1] did not observe scalable squeezing. We highlight favorable regions of the phase diagram to target in future experiments, and conclude with a discussion of new experimental directions with the potential to mitigate the effect of the positional disorder.

Model. — We consider the power-law interacting XXZ model

$$H = - \sum_{i < j} \frac{J}{r_{ij}^3} (\hat{s}_i^x \hat{s}_j^x + \hat{s}_i^y \hat{s}_j^y + \Delta \hat{s}_i^z \hat{s}_j^z) \quad (1)$$

with interaction coefficient J , anisotropy Δ , distance r_{ij} between spins i and j , and spin operators $\hat{s}_i^\alpha = \hat{\sigma}_i^\alpha / 2$ that obey the canonical commutation relations. The spins lie in a square 2D lattice of length L with lattice spacing a , which we set to unity, with each site occupied with probability $f = 1 - p$, where p is the vacancy probability. The average number of spins is therefore $N = fL^2$. We choose $1/r^3$ interactions as this is commonly realized in

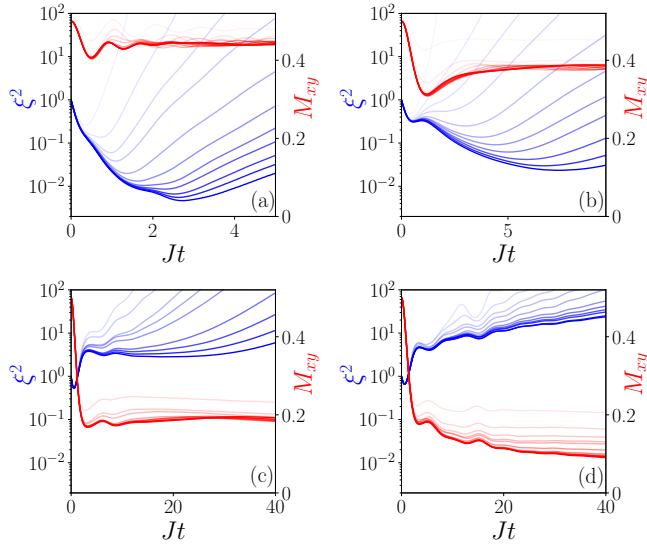


FIG. 1. Squeezing parameter ξ^2 (blue) and magnetization M_{xy} (red) vs time for different N values (faded lines) in the case of $\Delta = -1$. The results correspond to vacancy probability (a) $p = 0$, (b) $p = 0.5$, (c) $p = 0.75$, (d) $p = 0.85$. Darkness of lines scales with \sqrt{N} over a system size range of approximately $N \in \{10^2, 10^4\}$. Results correspond to an average over 10 disorder realizations with 6400 dTWA samples for each system.

experiments [26], including the recent NV experiment of Ref. [1]. The 2D geometry eliminates the angular dependence of the dipolar interaction. To characterize the squeezing we use the spin squeezing parameter [4, 6]

$$\xi^2 = \frac{N \min_{\mathbf{n} \perp x} \text{Var}[\mathbf{n} \cdot \hat{\mathbf{S}}]}{\langle \hat{S}^x \rangle^2} \quad (2)$$

where $\hat{S}^\alpha = \sum_i \hat{s}_i^\alpha$ is the collective spin and \mathbf{n} is the direction for which the variance is minimized in the plane perpendicular to the mean-spin vector, which we select as the x-direction. Scalable squeezing occurs when $\xi^2 \sim N^{-\nu}$, with $\nu \in \{0, 1\}$, ranging from the standard quantum limit ($\nu = 0$) to the Heisenberg limit ($\nu = 1$). In the disorder-free case, it has been shown that dynamics thermalizing to the easy-plane ferromagnetic ordered phase at late times display scaling $\xi_{\text{opt}}^2 \sim N^{-2/5}$ [10]. However, in practice this may only be observable for extremely large systems, before which one observes one-axis-twisting (OAT) scaling $\xi_{\text{opt}}^2 \sim N^{-2/3}$ [10]. Here, ξ_{opt}^2 is defined as the minimum value of the spin squeezing parameter during the time evolution, which represents the point of maximal metrological utility. Since the disorder preserves U(1) symmetry we expect a similar picture to hold here, with the critical temperature T_c lowering with increasing vacancy probability p .

We consider an initially x-aligned state $|\psi(0)\rangle = \prod_i^N |+\rangle_i$, which has a low enough energy density to ensure thermalization to the easy-plane ferromagnetic

phase in the disorder-free case (for $-4 \lesssim \Delta \leq 1$) [10]. We simulate Eq. (1) using the semi-classical method known as the discrete truncated Wigner approximation (dTWA) [27, 28], which in the disorder-free case yields near-exact results for sufficiently long-range power-law interactions – including the relevant case of $1/r^3$ – as shown in a recent comparison with tensor networks [29]. In the presence of strong disorder, this approximation is not expected to capture the dynamics of strongly interacting spins, as typically arises for a heavy-tailed distribution of effective interaction strengths $P(J^{\text{eff}})$ [10]. However, when spins are positioned on a regular lattice, a heavy-tailed distribution with interactions spanning orders of magnitude only emerges for $p \gtrsim 0.85$ [Fig. 2] [30]. The dTWA has previously been used for disordered systems to investigate spin dynamics with random Gaussian interactions [31], many-body-localized models [32], as well as explicit investigations of long-range dynamics with positional disorder both with [15, 33] and without [34, 35] an underlying lattice. Ref. [15] provided explicit results on the impact of finite filling fractions for the case of two-mode squeezing, with results suggesting a tolerance for disorder.

Spin squeezing with disorder.— In Fig. 1 we consider the case of $\Delta = -1$, which is relevant for NV centers in diamond [1]. We display results for the spin squeezing parameter ξ^2 (blue) and easy-plane magnetization $M_{xy} = \sqrt{\langle (\hat{S}^x)^2 + (\hat{S}^y)^2 \rangle}$ (red) vs time for different vacancy fractions p . Fig. 1(a) shows the disorder-free case ($p = 0$) for a range of system sizes (with increasingly faded lines for small systems), and clearly illustrate that the minimum squeezing parameter ξ_{opt}^2 decreases with system size, as expected for scalable squeezing, and observes similar scaling to the OAT model $\xi_{\text{opt}}^2 \sim N^{-2/3}$

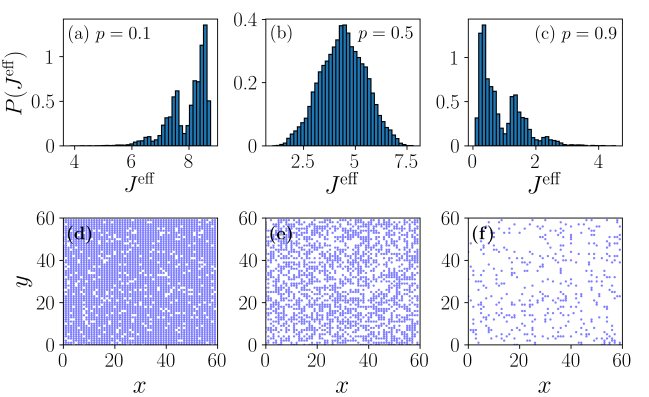


FIG. 2. Distribution of effective interaction strengths $P(J^{\text{eff}})$ for varying vacancy probability (a) $p = 0.1$, (b) $p = 0.5$, (c) $p = 0.9$. (d)-(f) Corresponding spatial positions of spins (dark points) in the 2D plane for a single disorder realization. Results in (a)-(c) are obtained from lattices with $N \sim \mathcal{O}(10^3) - \mathcal{O}(10^4)$, and are averaged over 25 disorder realizations.

[look ahead to Fig. 3(a) inset]. The magnetization quickly relaxes to a finite value, indicating thermalization to the ordered phase. Fig. 1(b) shows results for $p = 0.5$. While ξ_{opt}^2 is not as small as the disorder-free case, it still demonstrates a decrease with system size similar to the OAT scaling. Fig. 1(c) shows the $p = 0.75$ case. Here, the minimum occurs at early times on a scale set by the typical interaction strength and is not scalable. However, the second local minima does demonstrate scalable squeezing and for sufficiently large N [well beyond the maximum accessible $N \sim \mathcal{O}(10^4)$] will yield scalable squeezing. The time to reach this minimum also becomes large, which reflects the associated critical slowing down near the finite temperature phase boundary. Fig. 1(d) shows $p = 0.85$, which does not exhibit scalable squeezing. The magnetization is also seen to decrease with increasing system size. The magnetization reaches a quasi-steady state at late times (not shown, examples in SM [30]), which we denote by \bar{M}_{xy} , and decays as a power-law with increasing N , $\bar{M}_{xy} \sim N^{-\alpha}$, indicating thermalization to the disordered phase in the thermodynamic limit. Within the disordered phase, and away from the phase boundary, we find $\bar{M}_{xy} \sim N^{-1/2}$, in keeping with analytic behavior in L^{-1} .

These results can be qualitatively understood from the distribution of the effective interaction strengths $P(J^{\text{eff}})$, where $J_i^{\text{eff}} = \sum_j J r_{ij}^{-3}$, shown in Fig. 2 for a variety of p values. For weak disorder $p = 0.1$, Fig. 2(a), it can be seen that the largest J^{eff} values are approximately double that of the smallest values. In contrast, when $p = 0.9$ [Fig. 2(c)] this ratio becomes very large due to close pairs of spins having much stronger interactions than spins that are isolated in space – see Fig. 2(f) for the corresponding spatial distribution. For $p \approx 1$, the typical spacing between spins far exceeds the lattice spacing and the distribution acquires a very heavy tail, as noted in Ref. [1]. Nevertheless, this is not the case for moderate disorder such as $p = 0.5$ [Fig. 2(e)], which has no signatures of this heavy tail: all spins experience interactions of a comparable order of magnitude, which assists the persistence of collective squeezing behavior in Fig. 1.

Fig. 3(a) shows the optimal spin squeezing parameter ξ_{opt}^2 vs N for different p values (colors). The non-scalable minimum at early times that occurs for larger p values near the transition [as in Fig. 1(c) and (d)] complicates the analysis for the accessible system sizes. Following Ref. [10], we consider a more nuanced definition of ξ_{opt}^2 in which we only consider minima that reduce with the system size ($\nu > 0$) and diverge in time as $t_{\text{opt}} = N^\mu$ with $\mu > 0$ [30]. This has the effect of filtering out the irrelevant, non-scalable, minima. In the absence of a scalable minima we revert to the global minima. The results can be seen to track a power-law over at least an order of magnitude in N . Above a critical disorder strength $p = p_c$ we observe $\xi_{\text{opt}}^2 \sim N^0$ (const.). This is reflected in the inset, which shows the power-law ν vs p extracted

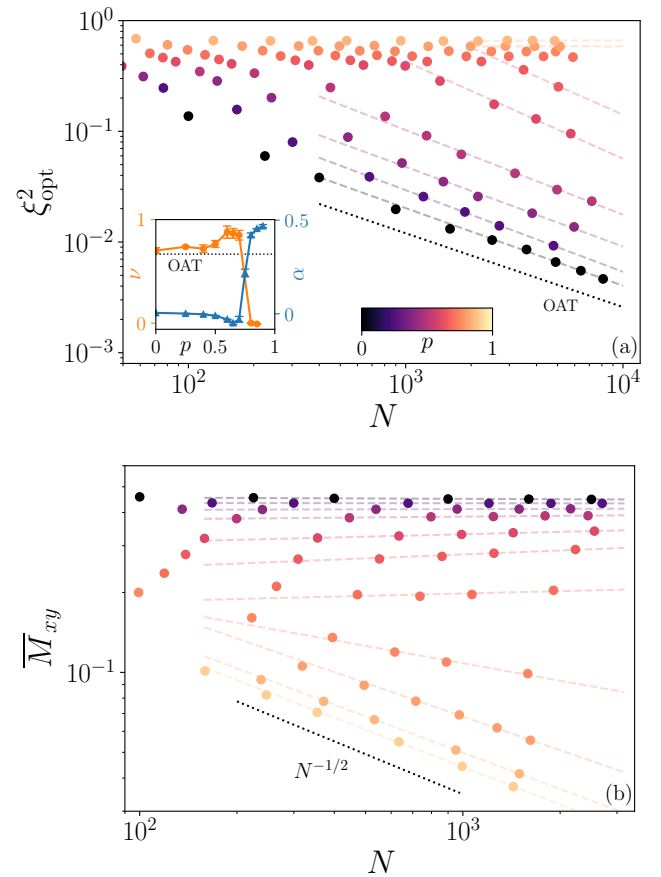


FIG. 3. (a) Optimal squeezing parameter ξ_{opt}^2 vs N for a range of vacancy probabilities p , where the colors range from $p = 0$ to $p = 0.85$ (legend) and we have set $\Delta = -1$. The dotted line gives the scaling for OAT: $\xi_{\text{opt}}^2 \sim N^{-2/3}$. Inset: ν (circles) vs p and α vs p (triangles), extracted from fits to the data in panels (a) and (b) respectively (dashed lines). Error bars indicate uncertainty of the fit. (b) Late-time magnetization \bar{M}_{xy} vs system size N for different p values [same legend as (a)]. Data in (a)[(b)] is obtained from an average over 10 (25) disorder realizations, with 6400 (1024) dTWA samples for each system.

from a log-log fit to the data. Near the transition, ν values larger than the OAT result of $\nu = 2/3$ are likely to be finite-size effects: even the disorder-free case shows a larger power-law for small N , only approaching OAT scaling at the larger system sizes we consider.

Since scalable squeezing occurs for dynamics thermalizing to the ordered phase, an alternate approach is to use the late-time magnetization \bar{M}_{xy} to diagnose the potential for scalable squeezing. In Fig. 3(b) we show \bar{M}_{xy} vs N for the same system. The data obeys a power-law $\bar{M}_{xy} \sim N^{-\alpha}$ for a range of p values (dashed-lines). In the inset of Fig. 3(a), we plot both α and ν , which take non-zero values in the disordered/ordered (scalable/non-scalable squeezing) phases respectively and both suggest a transition near $p_c \approx 0.7$. In the SM [30] we provide

similar data for an example with more points in the disordered phase ($\Delta = -2$), for which an extremely clean power-law scaling is visible.

Spin squeezing phase diagram.— We now look to establish a spin squeezing phase diagram in the $p - \Delta$ plane. Fig. 4(a) shows the finite-size magnetization exponent α , while Fig. 4(b) shows the spin squeezing exponent ν , where $\xi^2 \sim N^{-\nu}$. Both diagnostics predict a large region of scalable squeezing in the $p - \Delta$ plane, with increased robustness to disorder for the larger Δ values. We refrain from showing results in the region $0.5 < \Delta < 1$, where the ordered phase persists but the dynamics are extremely slow and spin squeezing occurs only at inaccessibly late times [30]. The slow dynamics are due to the proximity to $\Delta = 1$, where the initially x-aligned state is a ground-state (for all p), and hence no dynamics occur. Squeezing is also extremely robust to disorder in this region: even for $\Delta = 0.5$ we observe scalable squeezing for the entire simulated region $p \in \{0, 0.85\}$. This is due to the fact that disorder does not change the low energy behavior substantially near $\Delta = 1$, with the energy of states in adjacent magnetization sectors connected by raising and lowering operators mirroring the spectrum of the OAT model [12, 13] up to a correction from finite temperature fluctuations [10]. We refrain from presenting data for $p > 0.85$, as dTWA is less trustworthy here due to the heavy tailed interaction distribution. The phase diagram is suggestive that this region may display squeezing for $\Delta \gtrsim 0$.

While α and ν predict a qualitatively similar phase boundary, there are clear differences near the transition (blue dots vs red triangles). This is attributed to the absence of scalable squeezing in this region at the accessible system sizes, in analogy to the results in Fig. 1(c). We anticipate that the phase diagram in Fig. 4(a) is more accurate for $\Delta \leq -1$ as the magnetization data is less affected by finite-size corrections (beyond the $N^{-\alpha}$ scaling). However, for $\Delta > -0.5$ the magnetization typically does not fully converge to the steady state over accessible timescales [30]; in this region we take the largest times available (hatched region). Nevertheless, comparison with Fig. 4(b) shows scalable squeezing for the majority of these parameters.

Discussion.— The results in Fig. 4 illustrate why the recent NV experiment in Ref. [1] did not observe scalable squeezing: the strong disorder (p close to unity) far exceeded the critical value $p_c = 0.72(3)$ for $\Delta = -1$.

A promising way to make scalable spin squeezing more realistic in defect ensembles is to engineer a near-ordered sensor lattice through controlled defect creation. One practical route is to use electron-beam lithography to define a nanoscale patterned implantation mask, then perform nitrogen ion implantation and thermal annealing to create NV centers. NV creation at each site is inherently stochastic and can be approximated as a Poisson process. The implantation dose can be adjusted to target an av-

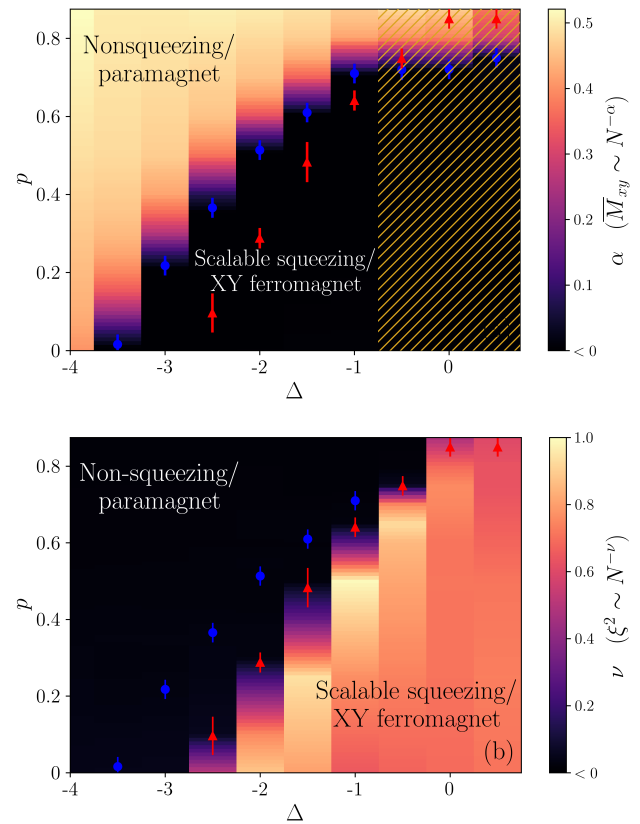


FIG. 4. (a) Scaling exponent α (color) as a function of vacancy fraction p and anisotropy Δ , where $\bar{M}_{xy} \sim N^{-\alpha}$. (b) Squeezing exponent ν (color) as a function of vacancy fraction p and anisotropy Δ , where $\xi^2 \sim N^{-\nu}$. Blue dots correspond to estimates of the phase boundary from α [data in (a)], while red triangles correspond to the estimate from ν [data in (b)]. Results in (a) [(b)] correspond to an average of 25 disorder realizations and 1024 (12800) dTWA samples for each system. Error bars include sampling uncertainty and discreteness of simulated p -grid [30]. Color data in the y -direction is linearly interpolated. For $\Delta = 0$ and $\Delta = 0.5$, red triangles represent a lower bound of $p_c = 0.85$ since we see scalable squeezing ($\nu > 0$) for the entire p -grid. Hatched region in (a) indicates simulations where the magnetization has not fully converged to the steady-state, in which data is taken for the largest times available.

erage of about one NV per lattice site. If the created NVs stay near the center of each site, then sites with multiple spins can be removed from their strong dipolar interaction via frequency resolved shelving or adiabatic depolarization, as outlined in Ref. [1]. Under this assumption, the “useful” sites are the ones with exactly one NV, while both empty sites and multi-occupied sites effectively behave like vacancies/inactive sites. With a Poisson mean of one, the probability of getting exactly one NV at a site is $e^{-1} \approx 0.37$, with effective vacancy probability $p = 1 - 0.37 = 0.63$. For $\Delta = -1$ this is expected to be in the scalable squeezing phase [Fig. 4 (a)].

An intriguing alternative experimental platform is the

boron vacancy (V_B) center in hexagonal boron nitride (hBN) [36–38]. Compared to NV in diamond, V_B defects may offer a key advantage for scalable squeezing: the defect is structurally simpler (a single missing boron atom), and the two-dimensional host makes it possible to create and visualize individual defects at the nanoscale using scanning transmission electron microscopy (STEM) [39]. If defect placement can be made deterministic, this approach could overcome the stochastic Poisson statistics and enable a near-ordered defect lattice with an effective vacancy fraction well below 0.63, which would be even more favorable for accessing the scalable squeezing regime.

Our results also suggest that only large lattices may realize a practical squeezing advantage close to the phase boundary. This is irrelevant for NVs and other solid-state platforms with typical atom numbers of $N \sim \mathcal{O}(10^{12})$, but should not be neglected in quantum gas experiments with arrays of size $N \sim \mathcal{O}(10^2 - 10^5)$ spins. Due to the disorder averaging, we are unable to reach the system sizes realized in Ref. [10] for the disorder free case, which sees a cross-over to $\nu = 2/5$ for $N > \mathcal{O}(10^4)$. Since these atom numbers are experimentally relevant, future work should interrogate this further for the disordered case.

Finally, our results lend weight to the suggestion of Ref. [1] that Floquet engineering techniques [40] be employed to engineer Δ values deep in the ordered phase, where we find squeezing to be highly robust to disorder. Operating close to the point $\Delta = 1$ may require careful consideration of system coherence times, due to the long evolution required to reach the squeezing minima.

Our work establishes the robustness of scalable squeezing to disorder in power-law interacting XXZ models. This is relevant for a large range of quantum simulation platforms, and provides a crucial step towards realizing quantum devices that yield a practical metrological advantage via spin squeezing. We also explain the absence of scalable squeezing in a recent NV experiment [1], provide potential strategies for disorder reduction, and highlight regimes with the best disorder tolerance.

Acknowledgments.— We acknowledge support from the NSF through awards OMR-2228725 (S.E.B. and M.H.K.) and DMR-1945529 (M.H.K.), and thank the High Performance Computing facility at The University of Texas at Dallas (HPC@UTD) for providing computational resources (S.E.B. and B. G.). C.Zu. acknowledges support from the NSF under Grant No. 2514391. C.Zh acknowledges support from Air Force Office of Scientific Research under Grant No. FA9550-2010220 and from NSF OSI-2503230. B. G. acknowledges funding in part by the Austrian Science Fund (FWF) Grant-DOI: 10.55776/PAT3563424.

During the preparation of this manuscript, a pre-print [41] appeared also demonstrating the effects of disorder on spin squeezing for the power-law interacting XXZ

model on the 2D lattice. Our results support the conclusions of that work. They obtain the finite-temperature phase diagram via quantum Monte Carlo simulations, obtaining results that are qualitatively similar, with possible quantitative agreement with our results for intermediate Δ values.

* samuel.begg@utdallas.edu

- [1] W. Wu, E. J. Davis, L. B. Hughes, B. Ye, Z. Wang, D. Kufel, T. Ono, S. A. Meynell, M. Block, C. Liu, *et al.*, Spin squeezing in an ensemble of nitrogen–vacancy centres in diamond, *Nature* **646** (2025).
- [2] C. L. Degen, F. Reinhard, and P. Cappellaro, Quantum sensing, *Rev. Mod. Phys.* **89**, 035002 (2017).
- [3] L. Pezzè, A. Smerzi, M. K. Oberthaler, R. Schmied, and P. Treutlein, Quantum metrology with nonclassical states of atomic ensembles, *Rev. Mod. Phys.* **90**, 035005 (2018).
- [4] D. J. Wineland, J. J. Bollinger, W. M. Itano, F. L. Moore, and D. J. Heinzen, Spin squeezing and reduced quantum noise in spectroscopy, *Phys. Rev. A* **46**, R6797 (1992).
- [5] M. Kitagawa and M. Ueda, Squeezed spin states, *Phys. Rev. A* **47**, 5138 (1993).
- [6] D. J. Wineland, J. J. Bollinger, W. M. Itano, and D. J. Heinzen, Squeezed atomic states and projection noise in spectroscopy, *Phys. Rev. A* **50**, 67 (1994).
- [7] J. Ma, X. Wang, C.-P. Sun, and F. Nori, Quantum Spin Squeezing, *Phys. Rep.* **509**, 89 (2011).
- [8] M. Foss-Feig, Z.-X. Gong, A. V. Gorshkov, and C. W. Clark, Entanglement and spin-squeezing without infinite-range interactions, arXiv preprint arXiv:1612.07805 .
- [9] M. A. Perlin, C. Qu, and A. M. Rey, Spin Squeezing with Short-Range Spin-Exchange Interactions, *Phys. Rev. Lett.* **125**, 223401 (2020).
- [10] M. Block, B. Ye, B. Roberts, S. Chern, W. Wu, Z. Wang, L. Pollet, E. J. Davis, B. I. Halperin, and N. Y. Yao, Scalable spin squeezing from finite-temperature easy-plane magnetism, *Nat. Physics* **20**, 1575 (2024).
- [11] T. Roscilde, F. Caleca, A. Angelone, and F. Mezzacapo, Scalable Spin Squeezing from Critical Slowing Down in Short-Range Interacting Systems, *Phys. Rev. Lett.* **133**, 210401 (2024).
- [12] T. Comparin, F. Mezzacapo, and T. Roscilde, Robust spin squeezing from the tower of states of U(1)-symmetric spin hamiltonians, *Phys. Rev. A* **105**, 022625 (2022).
- [13] T. Roscilde, T. Comparin, and F. Mezzacapo, Entangling Dynamics from Effective Rotor–Spin-Wave Separation in U(1)-Symmetric Quantum Spin Models, *Phys. Rev. Lett.* **131**, 160403 (2023).
- [14] T. Bilitewski and A. M. Rey, Manipulating Growth and Propagation of Correlations in Dipolar Multilayers: From Pair Production to Bosonic Kitaev Models, *Phys. Rev. Lett.* **131**, 053001 (2023).
- [15] A. Duha and T. Bilitewski, Two-mode squeezing in Floquet-engineered power-law interacting spin models, *Phys. Rev. A* **109**, L061304 (2024).
- [16] A. Duha, S. E. Begg, and T. Bilitewski, Nonequilibrium Critical Scaling of a Squeezing Phase Transition, *Phys. Rev. Lett.* **135**, 150401 (2025).
- [17] N. U. Koyluoglu, S. V. Rajagopal, G. L. Moreau, J. A. Hines, O. Marković, and M. Schleier-Smith, Squeezing

Towards the Heisenberg Limit with Locally Interacting Spins, arXiv preprint arXiv:2506.16973 .

[18] G. Bornet, G. Emperauger, C. Chen, B. Ye, M. Block, M. Bintz, J. A. Boyd, D. Barredo, T. Comparin, F. Mezzacapo, T. Roscilde, T. Lahaye, N. Y. Yao, and A. Browaeys, Scalable spin squeezing in a dipolar rydberg atom array, *Nature* **621**, 728 (2023).

[19] W. J. Eckner, N. Darkwah Oppong, A. Cao, A. W. Young, W. R. Milner, J. M. Robinson, J. Ye, and A. M. Kaufman, Realizing spin squeezing with rydberg interactions in an optical clock, *Nature* **621**, 734 (2023).

[20] J. A. Hines, S. V. Rajagopal, G. L. Moreau, M. D. Wahrman, N. A. Lewis, O. Marković, and M. Schleier-Smith, Spin Squeezing by Rydberg Dressing in an Array of Atomic Ensembles, *Phys. Rev. Lett.* **131**, 063401 (2023).

[21] J. Franke, S. R. Muleady, R. Kaubruegger, F. Kranzl, R. Blatt, A. M. Rey, M. K. Joshi, and C. F. Roos, Quantum-enhanced sensing on optical transitions through finite-range interactions, *Nature* **621**, 740 (2023).

[22] Y. K. Lee, M. Block, H. Lin, V. Fedoseev, P. J. Crowley, N. Y. Yao, and W. Ketterle, Observation of Spin Squeezing with Contact Interactions in One-and Three-Dimensional Easy-Plane Magnets, *Phys. Rev. Lett.* **135**, 023402 (2025).

[23] A. Douglas, V. Kaxiras, L. Su, M. Szurek, V. Singh, O. Marković, and M. Greiner, Spin Squeezing with Itinerant Magnetic Dipoles, *Phys. Rev. X* **15**, 041021 (2025).

[24] C. Miller, A. N. Carroll, J. Lin, H. Hirzler, H. Gao, H. Zhou, M. D. Lukin, and J. Ye, Two-axis twisting using Floquet-engineered XYZ spin models with polar molecules, *Nature* **633**, 332 (2024).

[25] C. Luo, H. Zhang, A. Chu, C. Maruko, A. M. Rey, and J. K. Thompson, Hamiltonian engineering of collective XYZ spin models in an optical cavity, *Nat. Phys.* **21**, 916 (2025).

[26] N. Defenu, T. Donner, T. Macrì, G. Pagano, S. Ruffo, and A. Trombettoni, Long-range interacting quantum systems, *Rev. Mod. Phys.* **95**, 035002 (2023).

[27] J. Schachenmayer, A. Pikovski, and A. M. Rey, Many-Body Quantum Spin Dynamics with Monte Carlo Trajectories on a Discrete Phase Space, *Phys. Rev. X* **5**, 011022 (2015).

[28] B. Zhu, A. M. Rey, and J. Schachenmayer, A generalized phase space approach for solving quantum spin dynamics, *New J. Phys.* **21**, 082001 (2019).

[29] S. R. Muleady, M. Yang, S. R. White, and A. M. Rey, Validating Phase-Space Methods with Tensor Networks in Two-Dimensional Spin Models with Power-Law Interactions, *Phys. Rev. Lett.* **131**, 150401 (2023).

[30] See Supplemental Material at [URL will be inserted by publisher], which includes additional details on error analysis, cTWA comparisons, and additional data.

[31] S. P. Kelly, A. M. Rey, and J. Marino, Effect of Active Photons on Dynamical Frustration in Cavity QED, *Phys. Rev. Lett.* **126**, 133603 (2021).

[32] O. L. Acevedo, A. Safavi-Naini, J. Schachenmayer, M. L. Wall, R. Nandkishore, and A. M. Rey, Exploring many-body localization and thermalization using semiclassical methods, *Phys. Rev. A* **96**, 033604 (2017).

[33] J. P. Covey, L. De Marco, Ó. L. Acevedo, A. M. Rey, and J. Ye, An approach to spin-resolved molecular gas microscopy, *New J. Phys.* **20**, 043031 (2018).

[34] A. Signoles, T. Franz, R. Ferracini Alves, M. Gärttner, S. Whitlock, G. Zürn, and M. Weidmüller, Glassy Dynamics in a Disordered Heisenberg Quantum Spin System, *Phys. Rev. X* **11**, 011011 (2021).

[35] P. Schultzen, T. Franz, C. Hainaut, S. Geier, A. Salzinger, A. Tebben, G. Zürn, M. Gärttner, and M. Weidmüller, Semiclassical simulations predict glassy dynamics for disordered Heisenberg models, *Phys. Rev. B* **105**, L100201 (2022).

[36] A. Gottscholl, M. Kianinia, V. Soltamov, S. Orlinskii, G. Mamin, C. Bradac, C. Kasper, K. Krambrock, A. Sperlich, M. Toth, *et al.*, Initialization and read-out of intrinsic spin defects in a van der waals crystal at room temperature, *Nat. Mater.* **19**, 540 (2020).

[37] R. Gong, X. Du, E. Janzen, V. Liu, Z. Liu, G. He, B. Ye, T. Li, N. Y. Yao, J. H. Edgar, *et al.*, Isotope engineering for spin defects in van der waals materials, *Nat. Commun.* **15**, 104 (2024).

[38] S. Biswas, G. Scuri, N. Huffman, E. I. Rosenthal, R. Gong, T. Poirier, X. Gao, S. Vaidya, A. J. Stein, T. Weissman, *et al.*, Quantum sensing with a spin ensemble in a two-dimensional material, arXiv preprint arXiv:2509.08984 (2025).

[39] J. Kikkawa, C. Shunei, J. Chen, Y. Masuyama, Y. Yamazaki, T. Mizoguchi, K. Kimoto, T. Taniguchi, and T. Teraji, Observation of boron vacancy concentration in hexagonal boron nitride at nanometer scale, *Nano Letters* **25**, 13191 (2025).

[40] J. Choi, H. Zhou, H. S. Knowles, R. Landig, S. Choi, and M. D. Lukin, Robust Dynamic Hamiltonian Engineering of Many-Body Spin Systems, *Phys. Rev. X* **10**, 031002 (2020).

[41] A. Kaplan-Lipkin, P. J. Crowley, J. N. Hallén, Z. Wang, W. Wu, S. Chern, C. R. Laumann, L. Pollet, and N. Y. Yao, Theory of Scalable Spin Squeezing with Disordered Quantum Dipoles, arXiv preprint arXiv:2512.19781 .

Supplemental Material for “Scalable Spin Squeezing in Power-Law Interacting XXZ Models with Disorder”

Samuel E. Begg,¹ Bishal K. Ghosh,^{1,2} Chong Zu,^{3,4} Chuanwei Zhang,^{3,4} and Michael Kolodrubetz¹

¹*Department of Physics, The University of Texas at Dallas, Richardson, Texas 75080, USA*

²*Institute of Physics, University of Graz, Universitätsplatz 5, 8010 Graz, Austria*

³*Department of Physics, Washington University, St. Louis, Missouri 63130, USA*

⁴*Center for Quantum Leaps, Washington University, St. Louis, Missouri 63130, USA*

(Dated: January 16, 2026)

NUMERICAL ERROR ANALYSIS

To estimate the error on our numerical results we need to consider both (a) dTWA sampling error and (b) disorder sampling error. For a given observable \hat{O} and a single disorder realization, we calculate the mean $\mathcal{O}_{\text{dtwa}}$ and the standard error of the mean σ_{dtwa} for the dTWA

samples. The full error after disorder averaging contains a direct contribution from the disorder average, $\sigma_{\text{dis}}^2 = \frac{1}{N(N-1)} \sum_s^N (\mathcal{O}_{\text{dtwa},s} - \bar{\mathcal{O}}_{\text{dtwa}})^2$, where the sum is over the sample index s and the bar denotes the disorder average over N samples. There is also a contribution from the dTWA error. These are combined to yield the total standard error of the mean

$$\sigma_{\text{SEM}} = \sqrt{\sigma_{\text{dis}}^2 + \sigma_{\text{dtwa}}^2}/N. \quad (\text{S1})$$

In the case of ξ^2 , the error is determined from error propagation of the individual errors for $\min_{\mathbf{n} \perp \mathbf{x}} \text{Var}[\mathbf{n} \cdot \hat{\mathbf{S}}]$ and $\langle \hat{S}^x \rangle^2$. Similarly, $(\hat{S}^x)^2$ are $(\hat{S}^y)^2$ correlated in the evaluation of \hat{M}_{xy} . For simplicity, we ignore this when obtaining our error estimate for the dTWA averaging of a single disorder sample. In particular, for the case of ξ^2 it requires evaluation for all considered angles in the plane $\mathbf{n} \perp \mathbf{x}$ (for a single trajectory). Additional details on the error analysis for the scaling exponents are contained in the following section.

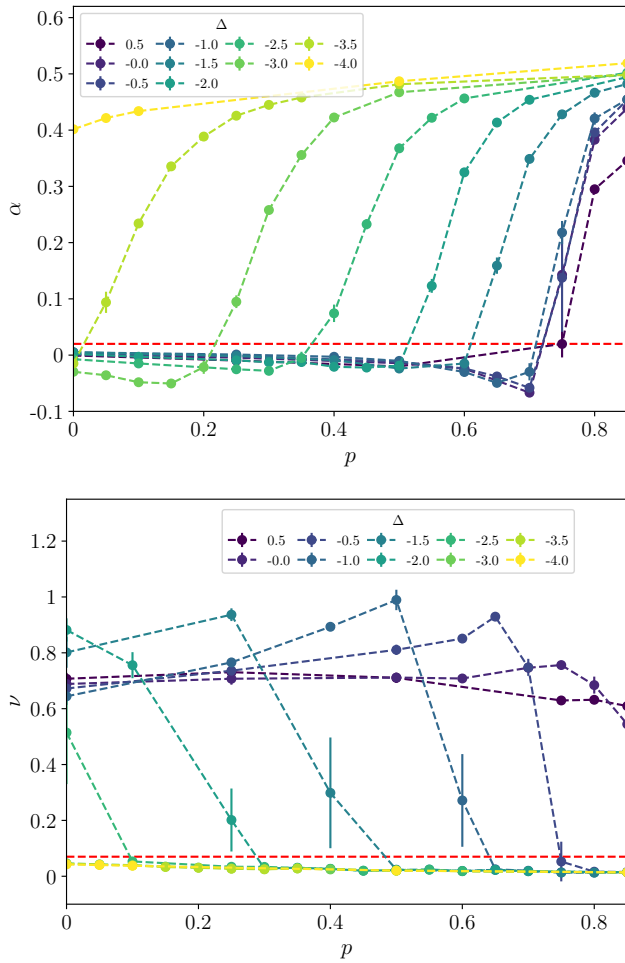


FIG. S1. (a) α vs p for a range of Δ values (legend). (b) ν vs p for a range of Δ values (legend). In both plots error bars the uncertainty is included as error bars, though these are small and hence not always visible in (a).

PHASE DIAGRAM DATA

As stated in the main text, in order to characterize the system size scaling of $\xi_{\text{opt}}^2 \sim N^{-\nu}$ we use a nuanced definition for the ordered phase, in which we only consider minima that scale non-trivially with the system size ($\nu > 0$) and occur at a time t_{opt} diverging with the system size $t_{\text{opt}} \sim N^\mu$, with $\mu > 0$. These definitions were used previously in Ref. [S1]. This combination allows us to filter out the non-scalable minima at early times, as is visible in the example of Fig. 1(c). In the absence of a minima fulfilling these requirements, as is typical in the disordered phase, we take the global minimum. Having established ξ_{opt}^2 and its uncertainty (via the procedure in the previous section), the exponent ν can be estimated via the power-law fit (in log-log space). We use a weighted linear least-squares fit, which also provides uncertainties by assuming the likelihood is Gaussian near the optimal point. In the vicinity of the transition, a scalable minima may only emerge for the largest system sizes [as in Fig. 1(c)]. If we do not observe at least three system sizes in this region, no exponent is estimated, since there is not enough data to establish a reasonable power-law fit. The exponent α is estimated from the late-time

magnetization (see the subsequent section) in a similar way, albeit without the subtleties.

Fig. S1 shows the exponents (a) α vs p and (b) ν vs p for a range of Δ values. This data is used to construct Fig. 4 of the main text. The red dashed lines indicate the threshold values that we use to determine the critical p values, p_c . Since we have data for a discrete set of p values, linear interpolation between the data points is used (lines between points) to yield this value. The extracted p_c are plotted as blue dots and red triangles in Fig. 4 of the main text. We also estimate the uncertainty in p_c from both the vertical error bars (dTWA and disorder error) and the discreteness of the simulated p grid in the x-direction. Since the discussion applies to both the magnetization [Fig. 4(a)] and spin squeezing parameter [Fig. 4(b)], we use an arbitrary exponent y as a proxy for α and ν in what follows. In order to estimate the error on p_c we first find the nearest points to the left (p_l) and right (p_r) the threshold respectively, with corresponding y -values $y_{l/r}$, and standard errors $\delta y_{l/r}$. The uncertainty in p_c , which we denote δp_c is derived from linear interpolation as

$$(\delta p_c)^2 = \left(\frac{p_r - p_l}{y_r - y_l} \right)^2 \{ t^2 (\delta y_l)^2 + (1-t)^2 (\delta y_r)^2 \} + \delta^2 \quad (\text{S2})$$

where $t = \frac{p_c - p_l}{p_r - p_l}$. Even without uncertainty in the y -direction, the true crossing could lie anywhere within the bracketing interval, and we have conservatively included half the interval width $\delta = (p_r - p_l)/2$ as an additional uncertainty.

LATE-TIME MAGNETIZATION

To calculate the late-time magnetization displayed in Fig. 3(b) and Fig. 4(a) of the main text, in the ordered phase we evolve for at least $\mathcal{O}(10)$ times longer than is needed to reach the spin squeezing minimum (t_{opt}) for the largest system sizes we consider. In the disordered phase we evolve for a comparably long time in units of J , although without reference to a time-scale associated with any spin squeezing minima. We extract the late-time magnetization \bar{M}_{xy} from an average over the final 10% of simulated times. Since the statistical errors across these times are correlated, we estimate the typical error from the average of the errors across the window. In many of our simulations, the results correspond to time-scales of order $Jt \sim \mathcal{O}(10^2)$ [see Fig. S2]. We typically take $\mathcal{O}(10)$ more samples when evaluating the spin squeezing parameter as compared to the magnetization; sample numbers are listed in the main text plots. This was chosen due to the smaller magnitude of ξ^2 , as well as the shorter times of interest.

Fig. S2 shows the magnetization evaluated to late times for the case of $\Delta = -2.0$ and (a) $p = 0.1$, (b)

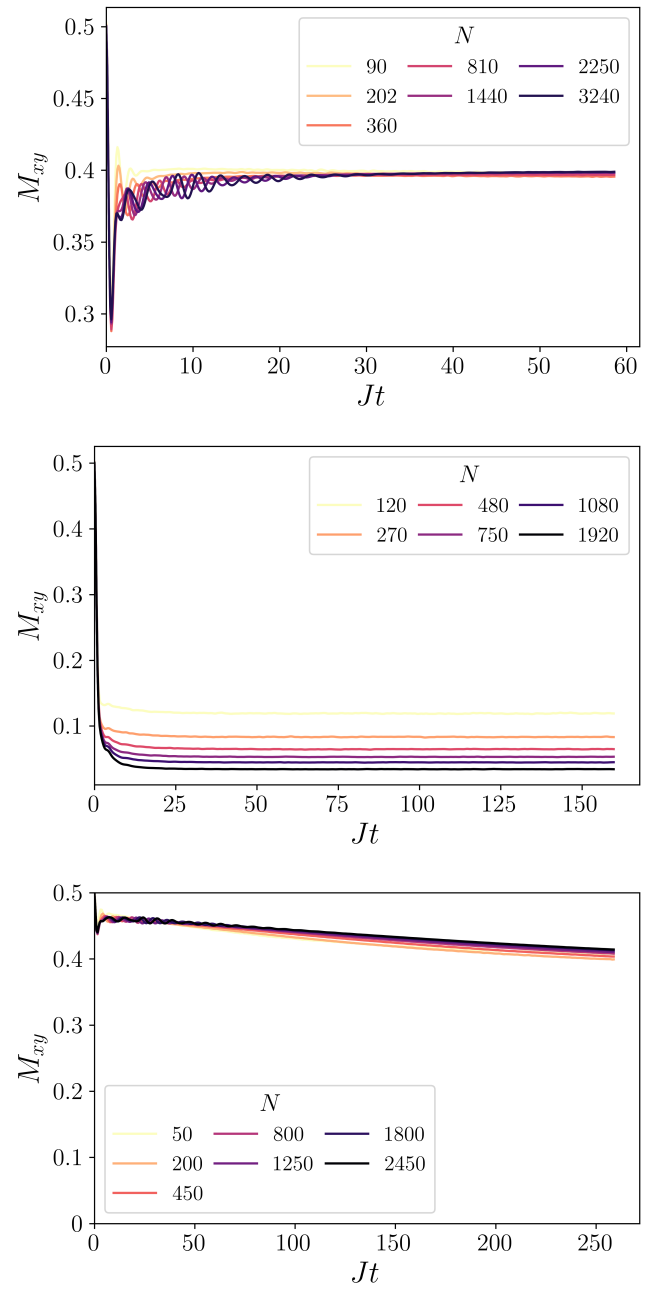


FIG. S2. Magnetization M_{xy} vs time for (a) $p = 0.1$ and (b) $p = 0.7$, for $\Delta = -2.0$. Data is shown for different system sizes; the disorder averaged system size $N = (1-p)L^2$ is shown in the legend. Data is obtained from an average over 25 disorder samples, with 1024 dTWA samples for each system. Error bars are included in the plot, but are very small and hence not visible. (c) Similar, but for $\Delta = 0$ with $p = 0.5$.

$p = 0.7$. The former is in the ordered phase, while the latter is in the disordered phase, as is visible from the scaling of the late time values with the system size. For $-0.5 \leq \Delta \leq 0.5$ the magnetization can relax very slowly, and does not always fully converge to the steady state over accessible times. In this region we consider the mag-

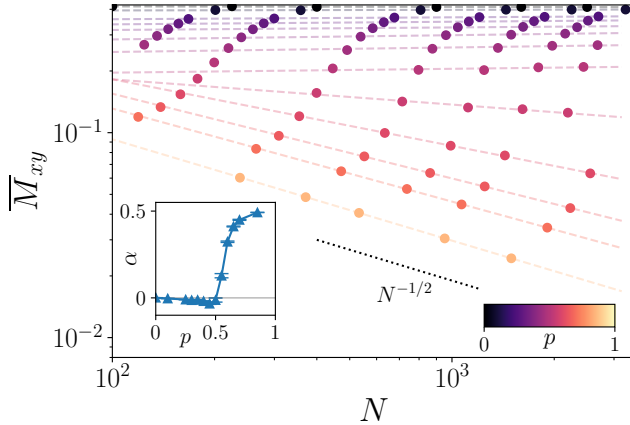


FIG. S3. Late-time magnetization \bar{M}_{xy} vs system size N for different p values (legend), for $\Delta = -2$. Data is obtained from an average over 25 disorder realizations, with 1024 dTWA samples for each system. Standard errors are included but are smaller than the symbol size and therefore not visible. Inset: α vs p , extracted from fits to the data in the main panel (dashed lines). Error bars indicate uncertainty of the fit.

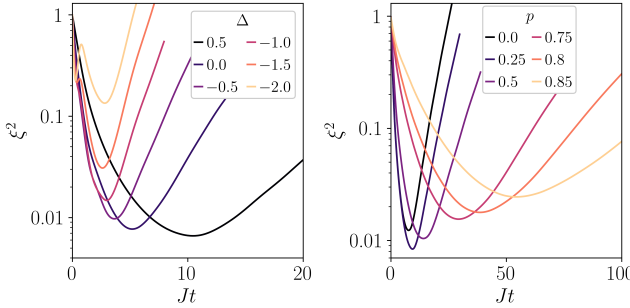


FIG. S4. Spin squeezing parameter ξ^2 vs time for varying Δ (legend), for constant $p = 0.25$ and $N = 1600$. Spin squeezing parameter ξ^2 vs time for $\Delta = 0.5$ for varying p . The data corresponds to N values in the range $N \in \{1450, 1850\}$, and is obtained from 25 disorder samples and 12800 dTWA samples.

netization at the longest available times. In Fig. 4(a) of the main text this region is indicated by the hatched region. An example of the slow relaxation is given in Fig. S2(c).

Fig. S3 shows \bar{M}_{xy} vs N in analogy to Fig. 3(b) in the main text, albeit for $\Delta = -2$. In this case there is more data in the disordered phase $p_c \approx 0.5$, and the non-trivial power-law scaling is observed for many p values. Larger p values are seen to approach $\bar{M}_{xy} \sim N^{-1/2}$ scaling.

ADDITIONAL DATA

In Fig. S4(a) we show the spin squeezing parameter vs time for a range of Δ values but constant system size $N = 1600$ and $p = 0.25$. The minima occurs at later times for the larger (more positive) Δ values. The time-scale for the dynamics will diverge on approach to $\Delta = 1$, since the initial state becomes an eigenstate and undergoes no dynamics. In Fig. S4(b) we consider the spin squeezing parameter vs time for the case of $\Delta = 0.5$, this time varying p . The data for the different p cases corresponds to similar system sizes in the range $N \in \{1450, 1850\}$. At larger p values the time-scale to reach the minimum also diverges, which is associated with critical slowing down on approach to the finite temperature phase transition. Based on the data in Fig. 4(b) of the main text, the critical value is in the region $p_c > 0.85$, which lies outside the parameters we simulate.

Fig. S5 shows the effective interaction strength distribution $P(J^{\text{eff}})$ for a range of p values, in analogy to Fig. 2 of the main text.

[S1] M. Block, B. Ye, B. Roberts, S. Chern, W. Wu, Z. Wang, L. Pollet, E. J. Davis, B. I. Halperin, and N. Y. Yao, Scalable spin squeezing from finite-temperature easy-plane magnetism, *Nat. Physics* **20**, 1575 (2024).

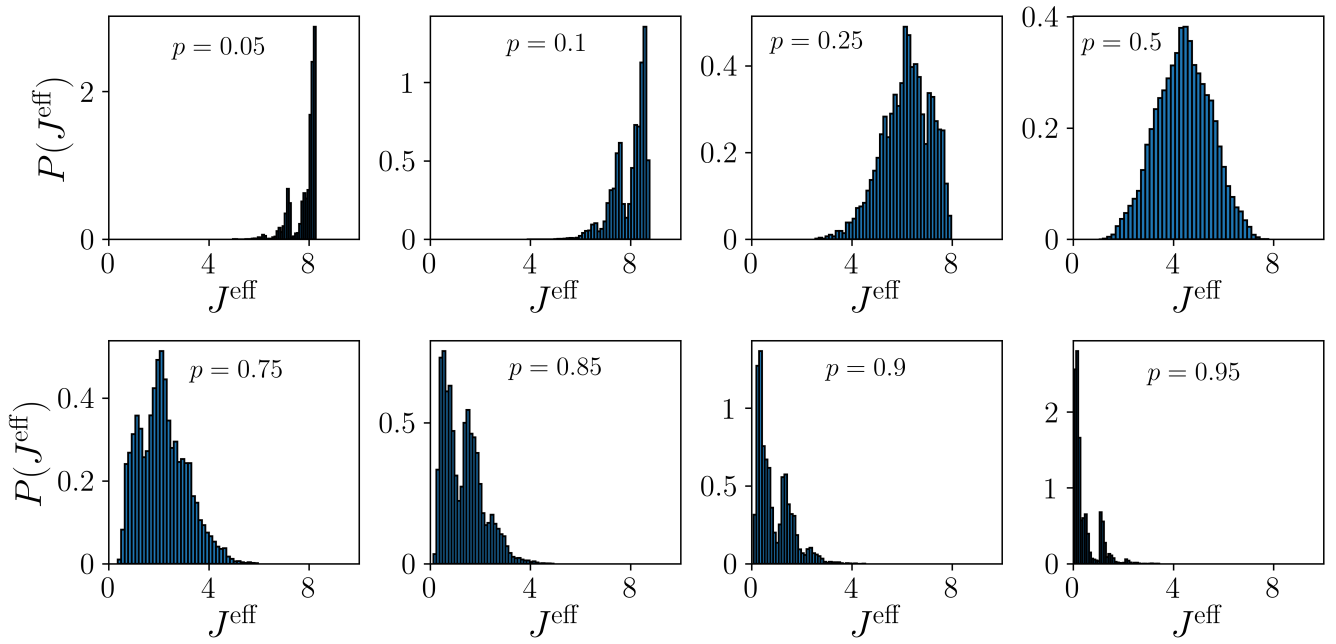


FIG. S5. Distribution of effective interaction strengths $P(J_{\text{eff}})$ for varying vacancy probability (labels). Data obtained from lattices with $N \sim \mathcal{O}(10^3) - \mathcal{O}(10^4)$ averaged over 25 disorder samples